

# Physics Behind the Oscillation of Pressure Tensor Autocorrelation Function for Nanocolloidal Dispersions

Tao Wang<sup>1,2</sup>, Xinwei Wang<sup>3,\*</sup>, Zhongyang Luo<sup>1</sup>, and Kefa Cen<sup>1</sup>

<sup>1</sup>State Key Laboratory of Clean Energy Utilization, Zhejiang University, Hangzhou 310027, P. R. China

<sup>2</sup>Department of Mechanical Engineering, N104 Walter Scott Engineering Center, The University of Nebraska-Lincoln, Lincoln, NE, 68588-0656, USA

<sup>3</sup>Department of Mechanical Engineering, 3027 H. M. Black Engineering Building, Iowa State University, Ames, IA 50011-2161, USA

In this work, extensive equilibrium molecular dynamics simulations are conducted to explore the physics behind the oscillation of pressure tensor autocorrelation function (PTACF) for nanocolloidal dispersions, which leads to strong instability in viscosity calculation. By reducing the particle size and density, we find the intensity of the oscillation decreases while the frequency of the oscillation becomes higher. Careful analysis of the relationship between the oscillation and nanoparticle characteristics reveals that the stress wave scattering/reflection at the particle-liquid interface plays a critical role in PTACF oscillation while the Brownian motion/vibration of solid particles has little effect. Our modeling proves that it is practical to eliminate the PTACF oscillation through suppressing the acoustic mismatch at the solid-liquid interface by designing special nanoparticle materials. It is also found when the particle size is comparable with the wavelength of the stress wave, diffraction of stress wave happens at the interface. Such effect substantially reduces the PTACF oscillation and improves the stability of viscosity calculation.

**Keywords:** Nanocolloidal Dispersion, Viscosity, Oscillation, Stress Wave Scattering, Particle-Liquid Interface.

In recent years, extensive research has been conducted on nanocolloidal dispersions which are heterogeneous mixtures consisting of very small particles with sizes typically in the order of 1–1000 nm. Because of the small size, large surface area, and significantly altered physical properties of nanoscale materials,<sup>1–3</sup> nanocolloidal dispersions have attracted considerable attention in applications related to cooling,<sup>4</sup> nanolubricant,<sup>5</sup> drug delivery and diagnosis.<sup>6,7</sup> In the application of nanocolloidal dispersions, the viscosity, which is related with the required pumping power and property of diffusion, plays a critical role in the delivery system. For confined microfluids, the viscosity can differ remarkably from that of the corresponding bulk fluids.<sup>8</sup> Several experimental work has been reported on the rheological behavior of nanocolloidal dispersions.<sup>9–12</sup> However, even for the same material, different viscosities have been reported.<sup>10,12,13</sup> It was pointed out that the large discrepancy could be due to differences in the dispersion techniques and differences in the size of the particles.<sup>10</sup> Rubio-Hernandez et al.<sup>11</sup> measured the pH value,  $\zeta$ -potential and intrinsic viscosity of the nanocolloidal dispersion and pointed out that the intrinsic viscosity

is related with the shape of clusters which are affected by many factors, including electroviscous effect, pH value, and shape of particles.

Several expressions<sup>11</sup> have been proposed to express the effect of nanoparticle volume fraction on the viscosity of hard particle suspensions. The experimental work barely reveals the physics behind the viscosity increase of nanocolloidal dispersions. Furthermore, because of the extremely small size of particles, it is difficult to characterize their dynamic rheological behavior experimentally. When the particle moves in a viscous fluid such as blood, the situation becomes more complicated.<sup>14</sup> To address the physics underlying the rheological behavior of nanocolloidal dispersions, several molecular dynamics (MD) methods have been developed over the years to explore the macroscopic transport properties of fluids, like self diffusivity and shear viscosity. There are two main categories of MD simulation for calculating the shear viscosity: equilibrium MD (EMD) and nonequilibrium MD (NEMD). The NEMD techniques usually involve measuring the macroscopic steady-state response of a system to a perturbing field and relating the linear response to a transport coefficient (e.g., Sllod algorithm).<sup>15,16</sup> Recently a new method using momentum impulse relaxation was

\* Author to whom correspondence should be addressed.

developed.<sup>17</sup> In this method, the shear viscosity is estimated by fitting the decaying coarse-grain Gaussian velocity profile. One major drawback of NEMD is that the shear viscosity is wavelength or box-size dependent.<sup>16</sup> In our extensive work using the momentum impulse relaxation method to calculate the shear viscosity of nanocolloidal dispersions, it is found that a very large system is needed. This will require a very long computational time, especially for low viscosity systems whose velocity distribution decays very slowly.

In EMD the viscosity is determined from pressure tensor ( $P_{\alpha\beta}$ ) fluctuations by using the Green-Kubo relation<sup>18,19</sup>  $\eta = V/(K_B T) \int_0^\infty \langle P_{\alpha\beta}(0)P_{\alpha\beta}(t) \rangle dt$ , where  $V$ ,  $K_B$  and  $T$  are volume, Boltzmann's constant and temperature, respectively.  $P_{\alpha\beta}$  is an off-diagonal ( $\alpha \neq \beta$ ) element of the pressure tensor given by  $P_{\alpha\beta} = (\sum_{i=1}^N p_{i\alpha} p_{i\beta} / m_i + \sum_i \sum_{j>i}^N r_{ij\alpha} F_{ij\beta}) / V$ , where  $N$ ,  $p_i$ ,  $r_{ij}$  and  $F_{ij}$  are the sum over all molecules, momentum vector for molecule  $i$ , the vector connecting the centers of molecules  $i$  and  $j$ , and the force between them, respectively. The advantage of EMD is its flexibility in the sense that a mixed system can be readily set up and more detail of transport coefficients or parameters, such as self-diffusion coefficient, shear viscosity or pressure tensor and stress wave propagation in the system can be studied. Nuevo et al.<sup>20</sup> used the EMD to study the self-diffusion coefficient and shear viscosity of nanocolloidal dispersions.<sup>20</sup> In their model the colloidal particles with diameters up to  $\sim 6$  times the solvent molecule were treated as solid bodies. These colloidal particles interacted with the solvent molecules following the Lennard-Jones (LJ) potential, and no internal atomic/molecular interaction is considered within the particle. Very high packing fractions (0.1–0.4) were studied. One significant problem found by the authors is that the shear viscosity is subject to greater statistical uncertainty with increasing packing fraction and colloidal particle size. Quite often it was difficult to establish a plateau value in the integration of time correlation function and the value of the viscosity decreased with increasing system size. In our attempt to calculate the viscosity of nanocolloidal dispersions by using EMD, strong oscillation in the autocorrelation function of the pressure tensor is observed while such phenomenon does not exist for pure fluids. This precludes precise determination of the viscosity for nanocolloidal dispersions.

Motivated to study the shear viscosity of nanocolloidal dispersions, this work reports the investigation into the physics behind the strong oscillation in the autocorrelation function of the pressure tensor. Argon liquids consisting of nanoparticles of different materials are studied. Through studying the effect of the size, mass/density and lattice constant of solid particles, it is found that the stress wave scattering/reflection at the particle-liquid interface gives rise to the strong oscillation in the autocorrelation function of the pressure tensor. Elimination of this oscillation

is achieved by adjusting the potential among atoms within nanoparticles to reduce the acoustic mismatch between particles and liquids.

In this work nanoscale solid particles are dispersed in the computational domain uniformly and the distance between particles is set the same initially. The liquid surrounding nanoparticles takes argon. In order to enhance the process of 'melting' for liquid argon at the initial stage of simulation, initially each argon atom is given a random Gaussian velocity distribution whose average is  $2(k_B T/m)^{1/2}$  where  $T$  is the expected equilibrium temperature. Periodical boundary conditions are applied along the three directions of the computational domain. The LJ potential ( $\phi_{ij}$ ) is applied to describe the interatomic interactions for atoms inside solid particles, liquid atoms and the interaction between solid and liquid atoms. The interaction energy between atoms  $i$  and  $j$ , separated by a distance  $r_{ij}$ , is  $\phi_{ij} = 4\epsilon_{s,l} [(\sigma_{s,l}/r_{ij})^{12} - (\sigma_{s,l}/r_{ij})^6]$ , where  $\epsilon$  and  $\sigma$  are the LJ well depth parameter and equilibrium separation parameter, separately. The subscripts  $s$  and  $l$  denote solid and liquid atoms. The typical combining Berthelot geometric mean rule  $\epsilon_{sl} = (\epsilon_s \cdot \epsilon_l)^{1/2}$  and Lorentz arithmetic mean combining rule  $\sigma_{sl} = (\sigma_s + \sigma_l)/2$  are applied for the potential between solid and liquid atoms.<sup>21</sup> The cutoff distance for MD simulation takes  $2.5 \sigma_l$  for liquid-liquid interaction, and  $2.5 \text{ Max} [\sigma_s, \sigma_l]$  for solid-solid and solid-liquid interactions. The half-step leap-frog scheme is used<sup>19</sup> in this work with a time step of 15 fs. Computation of the force between an atom and its neighbors is arranged by the cell structure and linked-list method.<sup>19</sup> It needs to be pointed out the system studied in this work is different from that by Nuevo et al.<sup>20</sup> In their work, each nanoparticle is treated as a single solid body (more like a large atom), and no interatomic interaction is considered within the particle. In this work, the structure and interatomic interaction within particles are considered. This makes it possible to reveal the physics behind the instability of viscosity calculation for nanocolloidal dispersions.

For purpose of comparing with literature values, the argon liquid is kept at a density of  $1.42 \text{ g} \cdot \text{cm}^{-3}$ . An equilibrium simulation is performed for 7000 steps ( $\sim 100$  ps) to make the system achieve an expected temperature of 143.4 K. The velocity scaling is performed for the solid and liquid separately and simultaneously. After the equilibrium calculation, the pressure of the whole domain stays at  $1.5 \sim 1.6 \times 10^8$  Pa. Then EMD simulation is performed for 150,000 steps ( $\sim 2$  ns) and the six pressure tensors  $P_{xx}$ ,  $P_{yy}$ ,  $P_{zz}$ ,  $P_{xy}$ ,  $P_{xz}$  and  $P_{yz}$  are calculated at each step. In order to improve the statistical stability of the shear viscosity result from the Green-Kubo relation, all the six pressure tensors are used. Since the system is isotropic at equilibrium, we have  $P_{\alpha\beta} = P_{\beta\alpha}$ .<sup>22</sup> Davis et al.<sup>23</sup> have shown that the shear viscosity can then be calculated from the integral  $\eta = V/(10 K_B T) \cdot \int_0^\infty \langle P^{os}(0) : P^{os}(t) \rangle dt$ , where  $P^{os}$  is

the symmetrical traceless pressure tensor with components  $P_{\alpha\beta}^{os}$  given by  $P_{\alpha\beta}^{os} = (P_{\alpha\beta} + P_{\beta\alpha})/2 - \delta_{\alpha\beta}(\sum_{\gamma} P_{\gamma\gamma})/3$ . For convenience of discussion,  $C_s(t)$  will be used to represent  $\langle P^{os}(0) : P^{os}(t) \rangle$  in our following discussions.

First of all, the size effect on the pressure tensor autocorrelation function (PTACF) is studied. The volume fraction of nanocolloidal particles is 3% for all the cases and 27 particles are configured in the physical domain. The potential for atoms within the solid particle shares the same parameters as that for argon except the well depth parameter.  $\epsilon_s$  takes 16  $\epsilon_l$  to prevent ‘melting’ of solid particles at high temperatures. After the equilibrium process, the lattice structure of the solid particle is very stable. In work by Nuevo et al.,<sup>20</sup> the oscillations were observed in the colloidal particle velocity autocorrelation function (VACF) and PTACF. In the pressure tensor, the movement of molecules is included. There are two possible reasons for the oscillation in the PTACF: oscillation of the particle and liquid, and stress wave reflection/scattering at the solid-liquid interface. Figure 1 presents how the oscillation in the PTACF varies with the particle size. It is observed there is a strong effect of particle size on the oscillation of PTACF which could significantly increase the statistical uncertainty in viscosity calculation. The PTACF curves oscillate with a higher frequency but dissipate more rapidly with the decreasing particle size. In work by Nuevo et al.,<sup>20</sup> it was mentioned that the oscillation frequency of VACF can be expressed by the Einstein frequency, which is the frequency at which any molecule would vibrate if it was undergoing small oscillations in the average potential well produced by its surrounding molecules. Particles with smaller size or lower density are known to have more rapid Brownian motion/oscillation in the liquid, and this is supposed to induce the oscillation in the PTACF. Figure 1 shows very little oscillation for the suspension with smaller particles (1 nm). This proposes that, with the decrease of particle size, although the increasing oscillation frequency of PTACF maybe is related with the faster

Brownian motion of particles, the oscillation intensity has very little to do with the particle oscillation. This leads to a conclusion that the oscillation in PTACF is not induced (or very little) by the oscillation of nanoparticles in the liquid. Simulations for pure liquid argon are also conducted, and no oscillation is observed in the PTACF.

The above conclusion is further explored and confirmed by another simulation by varying the particle density. The model solid material is changed to share the same parameters as copper except the atomic mass.  $\epsilon_s$  and  $\sigma_s$  take  $2.6756 \times 10^{-20}$  J and 2.315 Å, respectively.<sup>24</sup> The lattice constant  $a$  for copper crystal at 143.4 K is extrapolated as 3.606 Å considering the Gruneisen’s law.<sup>25</sup> The volume fraction of colloidal particles (1 nm radius) is also 3% for all the cases and 27 particles are configured in the simulation domain. Figure 2 presents the atomic mass/density effect on the PTACF. The atomic mass of liquid argon is  $6.63 \times 10^{-26}$  kg. For real copper the ratio  $m_s/m_l$  is 1.6, where  $m_s$  and  $m_l$  are the atomic mass of solid and liquid, separately. When  $m_s/m_l$  is equal to 0.295, the solid particle has the same density as the liquid argon. Figure 2 shows the PTACF curves are atomic mass/particle density dependent, oscillating with a higher frequency and damping with decreasing values of  $m_s/m_l$  (particle density). It is known that with the decrease of density, the solid particles are supposed to have stronger and faster vibration because of the Brownian motion. As mentioned above, if the oscillation of PTACF is directly related with the Brownian motion of nanoparticles, a stronger oscillation of PTACF should be found for lighter particles, especially when the solid particle has the same density as liquid. Actually, our simulation results show that the oscillation intensity of PTACF tends to be weaker with the decreasing of particle density. This proves the oscillation in the PTACF is not induced by the Brownian motion/oscillation of the nanoparticles. To explain this interesting phenomenon, the effect of stress wave scattering at the solid-liquid interface should be considered.

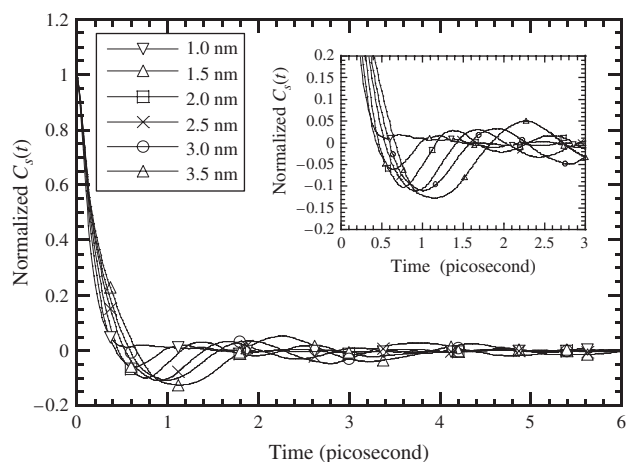


**Fig. 1.** The size effect on  $C_s(t)$  of nanocolloidal dispersions. The size shown in the figure is the particle radius.

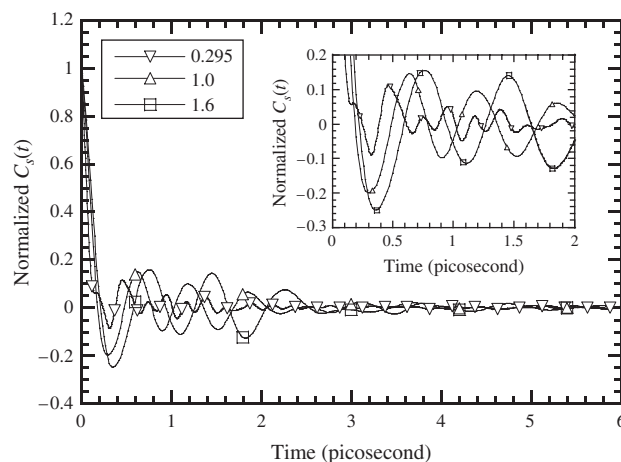


**Fig. 2.** The atomic mass effect on  $C_s(t)$  of nanocolloidal dispersions. The number shown in the figure is  $m_s/m_l$ .

It is well known that at the interface between dissimilar materials there will be an acoustic mismatch for stress wave/sound propagation. This acoustic mismatch is determined by the acoustic impedance  $Z = \rho \cdot c$ , where  $\rho$  and  $c$  are the mass density and sound speed, respectively. For a stress wave/sound traveling to the interface between materials  $A$  and  $B$ , the transmission coefficient is  $\alpha_{AB} = 4Z_A Z_B / (Z_A + Z_B)^2$ . The acoustic impedance mismatch at the nanoparticle-liquid interface in nanocolloidal dispersions will introduce a weak transmission and strong reflection/scattering of the sound/stress wave. The reflected or scattered stress wave from the interface will be reflected/scattered by other particle-liquid interface and forms oscillation between particles. Although the oscillation can occur inside the particles, this effect will be small compared with the oscillation in the liquid because of the small volume fraction of solid particles. If the oscillation of PTACF is induced by the stress wave, it is expected the oscillation in the PTACF can be eliminated through matching the acoustic impedance of the solid particles and liquid. In order to make the acoustic impedance match, one way is to change the density of particles but not changing the sound speed inside. This can be realized by using different lattice constants for the solid material, but keep the potential and atomic mass constant.

Before we explore the possibility of eliminating acoustic mismatch using the above strategy, NEMD simulation is carried out to study the sound speed in bulk solid by using different lattice constants. For the colloidal solid material at 143.4 K, our simulation results indicate that the stress wave travels at the same speed when the lattice constant is extended to  $1.0 \sigma_{Ar}$ ,  $1.2 \sigma_{Ar}$ ,  $1.35 \sigma_{Ar}$ ,  $1.5 \sigma_{Ar}$  and  $3.0 \sigma_{Ar}$ . For a simple system with the LJ potential, the sound velocity is only a function of  $\varepsilon$  and  $m$ , and is related to  $\sqrt{\varepsilon/m}$ . It is clear that the sound will travel at the same speed in bulk solid materials of different lattice constants if the well depth parameter and atomic mass are kept constant. Figure 3 shows the effect of the lattice constant on the oscillation of PTACF. The volume fraction of colloidal particles is still 3%,  $m_s/m_l(\alpha)$  takes 1, the particle radius is 2 nm, and  $\varepsilon_s$  takes  $16 \varepsilon_l$  for all the cases. The sound speed in solid particles is higher than that in liquid. In order to make the acoustic impedance match, the lattice constant should be extended to decrease the solid density. In order to keep the system stable, the equilibrium separation ( $\sigma_s$ ) and the lattice constant of the model solid material are extended with the same ratio. Figure 3 shows as the lattice constant of the solid particle is larger (less dense for the particle), the negative peak of PTACF curves decays very quickly with the decreasing density. When  $\alpha$  is 1.35, the PTACF curve is already quite smooth without visible oscillation. In this study, we conducted simulations for physical domains with one and 27 nanoparticles. Both cases showed very similar results. This confirms that even for systems with one nanoparticle, the system is still

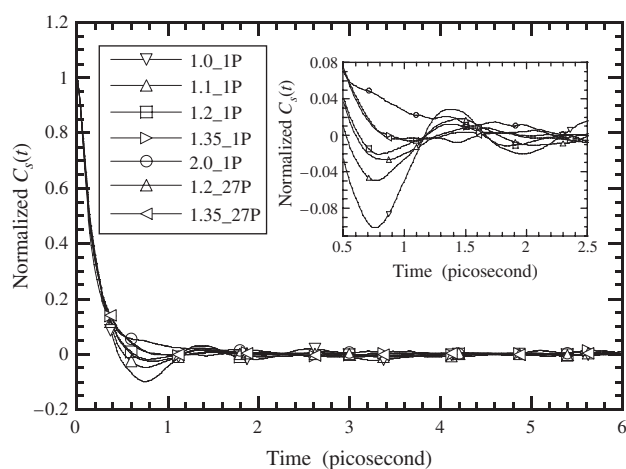


**Fig. 3.** The  $C_s(t)$  of nanocolloidal dispersions at different lattice constants for colloidal particles. The numbers shown in the figure is  $a_s/a_{Ar}$ . '1P' and '27' mean 1 and 27 solid particles in the simulation box.

large enough to achieve acceptable statistical uncertainty for EMD simulation.

The density effect on PTACF oscillation from Figures 2 and 3 proves one point: the sound speed in the colloidal particle is higher than that in the liquid and the decrease of particle density makes the acoustic impedance of the two materials match better. Elimination of this acoustic mismatch can completely suppress the oscillation in the PTACF, leading to the conclusion that the oscillation in the PTACF is induced by the stress wave reflection/scattering at the particle-liquid interface. Our NEMD simulations about the sound speed in bulk solid and liquid indicate that for the colloidal solid material at 143.4 K, the stress wave travels at a speed of  $6280 \text{ m} \cdot \text{s}^{-1}$  in the [100] direction when  $m_s/m_l(\alpha)$  takes 1 and the  $\varepsilon_s$  takes  $16 \varepsilon_l$ . For liquid argon at 143.4 K under pressure of  $1.5 \sim 1.6 \times 10^8 \text{ Pa}$ , the stress wave travels at a speed of  $1190 \text{ m} \cdot \text{s}^{-1}$ . When the acoustic impedance of the two materials is the same, the colloidal particle needs to have a smaller density, corresponding to a lattice constant of  $1.7 \sigma_l$ . From Figure 3 we observed that when  $\alpha$  is 1.35 and 2.0, the PTACF curve is already very smooth, meaning the reflection/scattering of the stress wave at the solid-liquid interface is substantially weak. To further confirm that the oscillation in Figure 3 is not induced by the particle oscillation, the VACF of particles is studied. The VACF of particles, denoted as  $C_v(t)$  in the following discussions, is the ensemble average of the product of particle's velocity  $v(t_0)$  and  $v(t_0 + t)$  over time origins. They share the same parameters and potentials as the simulations presented in Figure 3 and only one solid particle is used in the liquid. The results are summarized in Figure 4. It is observed when the lattice constant within the particle is extended to  $1.0 \sigma_{Ar}$ ,  $1.1 \sigma_{Ar}$  and  $1.2 \sigma_{Ar}$ , there are no oscillations for VACF curve while strong oscillations are found for PTACF (see Fig. 3). Only when the lattice constant is extended to  $2 \sigma_{Ar}$ , there is an obvious oscillation in the VACF curve which may be induced by

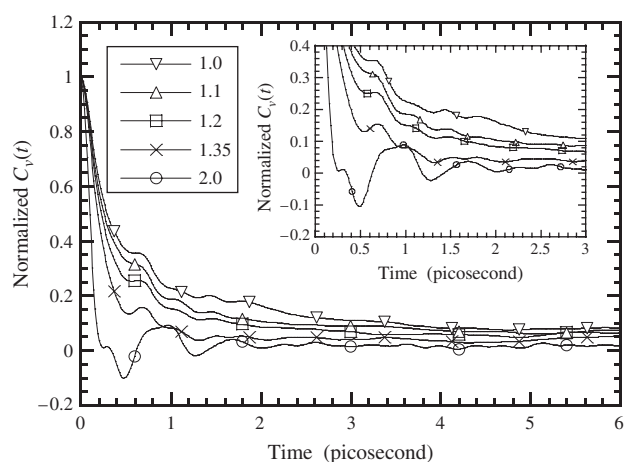


**Fig. 4.** The velocity autocorrelation function of colloidal nanoparticles with different lattice constants. The numbers shown in the figure is  $a_s/a_{Ar}$ .

the oscillation of the particle because of its low density. But no oscillation in the PTACF is observed (shown in Fig. 3). These results give solid evidence that the stress wave scattering/reflection largely induces the oscillation in the PTACF. Considering the very big system we studied (up to millions of atoms), the periodic boundary condition cannot induce the oscillation.

Another interesting phenomenon is that the oscillation frequency of the PTACF slightly increases with the decreasing size/density of particles as shown in Figures 1 and 2. Considering the above results and comparing with the mass effect on the colloidal particle VACF studied in work of Nuevo et al.,<sup>20</sup> it is conclusive that the quicker movement of particles with smaller size or density will induce more oscillation of the liquid/solid interface, which will directly affect the stress wave scattering/reflection at the interface. Especially at the same volume fraction of solid particles, the distance between particles will decrease quickly with the decreasing particle size. This will make the stress wave take shorter time to be reflected back-and-forth between particles. The particle size effect on the oscillation of the PTACF as shown in Figure 1 can also be explained by the stress wave scattering at the particle-liquid interface. When the stress wavelength and particle size are comparable, diffraction happens. This means more ‘forward scattering’ and less ‘back scattering’ although the acoustic impedance is not changed. That explains why the oscillation intensity decreases with the decreasing of the particle size at the same particle density. It is physically reasonable to conclude that when the particles become substantially small (just like the solvent atoms), no oscillation in the PTACF will be observed since no “back scattering” will occur.

In summary, EMD simulations were conducted to explore the physics behind the oscillation in the PTACF of nanocolloidal dispersions. Such oscillation usually leads to large instability in the viscosity calculation. It was

observed that the intensity of the oscillation decreased and the frequency of the oscillation slightly increased with the decreasing particle size and density. The effect of size and density of nanoparticles on PTACF showed the oscillation of PTACF was not directly related with the Brownian motion of nanoparticles. The stress wave scattering at the particle-liquid interface played a critical role in the oscillation of PTACF. This hypothesis was confirmed by eliminating the oscillation of PTACF through reducing the acoustic impedance mismatch between particles and liquid. For smaller particles whose size was comparable to the wavelength of stress wave, diffraction happened and the oscillation disappeared even when the acoustic impedance of the two materials has a large mismatch.

**Acknowledgments:** This work was supported by National Science Foundation (CMS: 0457471) and Nebraska Research Initiative. Partial support for this work from the start-up fund of Iowa State University is gratefully acknowledged. The authors especially appreciate the strong support from the China Scholarship Council for the State Scholarship Fund to pursue the research.

## References and Notes

1. J. Rupp and R. Birringer, *Phys. Rev. B* 36, 7888 (1987).
2. H. Gleiter, *Prog. Mater. Sci.* 33, 223 (1989).
3. H. Zhang and J. F. Banfield, *J. Mater. Chem.* 8, 2073 (1998).
4. J. A. Eastman, S. U. S. Choi, S. Li, W. Yu, and L. J. Thompson, *Appl. Phys. Lett.* 78, 718 (2001).
5. F. D. S. Marquis and L. P. F. Chibante, *JOM* 57, 32 (2005).
6. S. Jin and K. Ye, *Biotechnol. Prog.* 23, 32 (2007).
7. A. Komoto and S. Maenosono, *J. Chem. Phys.* 125, 114705 (2006).
8. J. Zhang, B. D. Todda, and K. P. Travis, *J. Chem. Phys.* 121, 10778 (2004).
9. J. Yamanaka, N. Ise, H. Miyoshi, and T. Yamaguchi, *Phys. Rev. E* 51, 1276 (1995).
10. X. Wang, X. Xu, and S. U. S. Choi, *J. Thermophys. Heat Trans.* 13, 474 (1999).
11. F. J. Rubio-Hernandez, M. F. Ayucar-Rubio, J. F. Velazquez-Navarro, and F. J. Galindo-Rosales, *J. Colloid and Interface Science* 298, 967 (2006).
12. N. Putra, W. Roetzel, and S. K. Das, *Heat Mass Trans.* 39, 775 (2003).
13. B. C. Pak and Y. I. Cho, *Exp. Heat Trans.* 11, 151 (1998).
14. M. Kim, D. Kim, S. Lee, M. S. Amin, I. Park, C. Kim, and M. Zahn, *IEEE Transactions on Magnetics* 42, 979 (2006).
15. D. J. Evans and G. P. Morris, *Statistical Mechanics of Nonequilibrium Liquids*, Academic, London (1990).
16. B. Hess, *J. Chem. Phys.* 116, 209 (2002).
17. G. Arya, E. J. Maginn, and H.-C. Chang, *J. Chem. Phys.* 113, 2079 (2000).
18. R. Zwanzig and R. D. Mountain, *J. Chem. Phys.* 43, 4464 (1965).
19. M. P. Allen and D. J. Tildesley, *Computer Simulations of Liquids*, Clarendon, Oxford (1987).
20. M. J. Nuevo, J. J. Morales, and D. M. Heyes, *Phys. Rev. E* 58, 5845 (1998).
21. R. L. Scott and D. V. Fenby, *Annu. Rev. Phys. Chem.* 20, 111 (1969).
22. L. I. Kioupis and E. J. Maginn, *J. Chem. Engg.* 74, 129 (1999).
23. P. J. Davis and D. J. Evans, *J. Chem. Phys.* 100, 541 (1994).
24. S. R. Phillpot, D. Wolf, and H. Gleiter, *J. Appl. Phys.* 78, 847 (1995).
25. G. B. Mitra and A. K. Giri, *J. Phys. D: Appl. Phys.* 19, 1065 (1986).

Received: 27 November 2007. Accepted: 26 April 2008.